



37

## 38 **Introduction**

39 For pharmaceutical applications tablets are the accepted and most widely used dosage form  
40 due to their being cost effective to manufacture, having relative ease of large scale of  
41 production, resulting product stability, related to the availability of reliable manufacture  
42 processes, and ability to provide correct reproducible dosage of drug from tablet to tablet and  
43 the convenience for patients [1, 2]. Critical quality attributes, such as disintegration time or  
44 amount of API dissolved after a certain time, are linked to their physical, mechanical, chemical,  
45 biological and also optical properties. During formation of a tablet, the mixture of drug and  
46 excipient particles is compacted, usually directly or following a granulation step, into a stable  
47 porous solid.

48 Historically, mechanical properties have played an important role in order to assess the  
49 functionality of a pharmaceutical tablet following the compaction step. Indentation, elasticity,  
50 tensile strength, brittle fracture index, bonding index, strain index, viscoelasticity,  
51 compressibility, compatibility, and tabletability are among the various mechanical properties  
52 of a tablet that have been explored in depth [3 - 8]. The mechanical properties of pharmaceutical  
53 tablets can be described by the relationship between the applied force during the compression  
54 and the resulting plastic deformation, and inter-particle bonding within the tablet [9]. These  
55 dictate the behaviour of pharmaceutical powder mixtures both during and after compaction.  
56 Stress and strain are the basic mechanical properties to describe the relationship between  
57 compressive pressure and the resulting deformation [8]. Compressibility (solid fraction as a  
58 function of compaction pressure) and compactibility (tensile strength in relation to solid  
59 fraction) [10] are terms commonly used to describe the densification and reduction in volume  
60 of a powder bed by the application of pressure alone, and both properties are considered to be  
61 the major parameters contributing to tabletability, defined as the dependence of tensile strength  
62 on compaction pressure [11]. In this study, we propose to establish an optical parameter that is  
63 related to the mechanical properties, such as the bulk modulus of pharmaceutical tablets. This  
64 topic of high importance in pharmaceutical sciences (see, for example, reference to strain [4 -  
65 8, 10] and compressibility [12 – 18]). In this study, the emphasis is on the research of the  
66 development of non-contact sensing and data analysis methods to quantify structural and  
67 mechanical properties of pharmaceutical tablets using terahertz (THz) time-delay measurement  
68 techniques [19].

69 Recently, we have introduced a novel structural parameter ( $S$ ), which describes the pattern of  
70 arrangement of different constituents in porous pharmaceutical tablets [20]. By pattern  
71 arrangement we mean the arrangement of drug and excipient constituting the skeletal-pore  
72 elements (solid phase) in series, parallel or a mix of both patterns. This structural parameter is  
73 assumed to play an important role both in the compressibility of a tablet, and in the description  
74 of the ingress and permeation of liquids in pharmaceutical tablets. In addition to developing  
75 the optical compressibility parameter, we consider in more detail the structural parameter  $S$  in  
76 respect to the explicit dependence of  $S$  on a range of various tablet properties, and analyse the  
77 correlation of the optical compressibility parameter with  $S$ .

78 This study continues our work to retrieve physical parameters, which directly affect critical  
 79 quality attributes of a tablet, from non-destructive and contactless terahertz measurements. So  
 80 far, we have established correlation between the effective THz refractive index and porosity  
 81 [21], surface roughness [21], lumped structural parameter [20], and Young's modulus [8].  
 82 Here, we suggest a new optical compressibility parameter and compare it with the measured  
 83 bulk modulus of tablets.

## 84 **Theory**

85 The data analysis in this study is based on the measurement of time delay ( $\Delta t$ ) of a terahertz  
 86 pulse. The time delay is caused by the more optically dense tablet compared to the undisturbed  
 87 propagation of the pulse through nitrogen gas, which is typically used as a reference medium  
 88 in laboratory terahertz measurements. Hence, we assume the validity of the following equation

$$89 \quad (n_{\text{eff}} - 1)H = c\Delta t \quad (1)$$

90 where  $n_{\text{eff}}$  is the effective refractive index of the tablet,  $H$  is the height of the round flat-faced  
 91 tablet, corresponding in direction to the normal of incidence, and  $c$  is the velocity of light in  
 92 vacuum. The refractive index of nitrogen is assumed to be equal to unity.

93 In the derivation of the structural parameter  $S$  of a porous pharmaceutical tablet we exploited  
 94 the concept of effective permittivity of the tablet and Wiener bounds that define the boundary  
 95 range for the effective permittivity in the absence of scattering of the terahertz waves. Aspnes  
 96 [22] provides a nice description of Wiener bounds for composite materials by considering two  
 97 limiting cases, namely no screening and maximum screening of microstructures in the direction  
 98 of the external electric field. This means that, for example, a needle-shaped particle orientated  
 99 parallel to the external electric field (in our case direction of propagation of the THz pulse)  
 100 would develop little screening, whereas a disc-shaped particle of the same volume would yield  
 101 strong screening. The effective permittivity of a porous pharmaceutical tablet can be assumed  
 102 to be constructed from parallel and series connections of the internal solid structures as follows  
 103 [20]:

$$104 \quad \varepsilon_{\text{eff}} = \frac{1}{\frac{1-S}{\varepsilon_U} + \frac{S}{\varepsilon_L}} \quad (2)$$

105 where  $\varepsilon_U$  and  $\varepsilon_L$  are the upper and lower Wiener bounds of the permittivity, respectively, and  
 106  $S$  is the structural parameter.  $S$  is a measure of that fractional part of the randomly distributed  
 107 structures in a porous medium that can be lumped together in parallel and in series coordination,  
 108 respectively. Since the true value of the effective permittivity of the tablet is always confined  
 109 between the upper and lower values of the effective permittivity, the structural parameter  $S$  is  
 110 a number that ranges from zero (all constituents in parallel) to one (all constituents in series).  
 111 The definition of  $S$  holds equally for multiphase systems. In our study, we will only deal with  
 112 a three-phase system, air and two solid phases, respectively. Eq. (2) was originally defined for  
 113 effective heat conductivity [23] of porous media, such as coated paper products, but for the  
 114 sake of analogy we have modified the concept for this analogous case, namely to represent the  
 115 effective permittivity of porous media.

116 In the case of a three-phase system, such as air (or nitrogen gas), micro-crystalline cellulose  
 117 (MCC) and active pharmaceutical ingredients (API) in this study, the equations for the upper  
 118 and lower Wiener bounds of the effective refractive index are as follows:

$$119 \quad n_U^2 = f_{\text{air}} + f_{\text{MCC}}n_{\text{MCC}}^2 + f_{\text{API}}n_{\text{API}}^2 \quad (3)$$

120

121 and

$$122 \quad \frac{1}{n_L^2} = f_{\text{air}} + \frac{f_{\text{MCC}}}{n_{\text{MCC}}^2} + \frac{f_{\text{API}}}{n_{\text{API}}^2} \quad (4)$$

123 where  $f_{\text{air}}$ ,  $f_{\text{MCC}}$  and  $f_{\text{API}}$  are the volume fractions of air (i.e. the pores constituting the tablet  
 124 porosity), MCC and API, respectively. The symbols  $n_{\text{MCC}}$  and  $n_{\text{API}}$  denote the intrinsic  
 125 refractive indices of MCC and API. If we apply the well-known relation from optics for the  
 126 real relative permittivity and the refractive index of a non-absorbing insulating medium,  
 127 namely,  $n = \sqrt{\varepsilon}$ , we get from Eqs. (2)-(4) the expression

$$128 \quad S = \frac{1}{n_U^2 - n_L^2} \left[ \frac{n_U^2 n_L^2}{n_{\text{eff}}^2} - n_L^2 \right] \quad (5)$$

129 In the pharmaceutical industry, the compressibility of pharmaceutical tablet formulations is an  
 130 important factor which determines the required applied force on the composition of powder  
 131 mixture to turn it into a structurally stable porous tablet. It greatly affects a range of tablet  
 132 properties such as disintegration, dissolution, structural integrity, bioavailability and  
 133 absorption as well as the mechanical properties, such as hardness and friability. The  
 134 compressibility is defined as a mechanical property, which describes the relationship between  
 135 the resulting compact density or strength (hardness / friability) and the compaction pressure  
 136 [24].

137 We propose an “optical compressibility” parameter to estimate the mechanical compressibility  
 138 of an excipient or complex formulation based on a simple analysis of the transmitted terahertz  
 139 pulse. This “optical compressibility” is defined by using Eq. (1) as an optical state equation in  
 140 analogy to the equation of state of a medium in thermodynamics. For the sake of clarity, we  
 141 first consider the simple thermodynamic equation of state of an ideal gas, which is defined with  
 142 the aid of the pressure ( $p$ ), volume ( $V$ ), absolute temperature ( $T$ ), the number of gas molecules  
 143 ( $\nu$ ) and the gas constant ( $R$ ) as  $pV = \nu RT$ . The optical state equation, namely Eq. (1), resembles  
 144 the mathematical form of the thermodynamic state equation of an ideal gas, but obviously has  
 145 different variables. The compressibility  $\beta$ , of an ideal gas is defined using the concept of a  
 146 partial derivative as follows:

$$147 \quad \beta = -\frac{1}{V} \left( \frac{\partial V}{\partial p} \right)_T = \frac{1}{p} \quad (6)$$

148 The unit of this compressibility is  $\text{Pa}^{-1}$ . A definition similar to Eq. (6) can be exploited also for  
 149 the compressibility of liquids and solids in the field of thermodynamics, but usually the state  
 150 equation is more complicated than that of an ideal gas. The interpretation of Eq. (6) states that

151 the higher the pressure, the lower is the value of the compressibility. In an analogous manner  
 152 to Eq. (6), we define with the aid of Eq. (1) the optical compressibility parameter as

$$153 \quad \beta_{THz} = -\frac{1}{H} \left( \frac{\partial H}{\partial n_{eff}} \right)_{\Delta t} = \frac{1}{n_{eff}-1} \quad (7)$$

154 The dimensionless optical compressibility defined in this way shows inverse dependence of  
 155 the compressibility on the effective refractive index, which in turn is linearly correlated to the  
 156 density/porosity of the tablet. The interpretation of Eq. (7) is that the denser the medium (i.e.  
 157 higher compaction pressure) the higher the effective refractive index, since the density of a  
 158 medium is correlating with the refractive index of the medium, and, hence, the lower the optical  
 159 compressibility parameter.

160 Next, we wish to have a more detailed picture regarding the behaviour of the optical  
 161 compressibility parameter defined in Eq. (7). For this purpose, we consider an estimate for the  
 162 explicit dependence of the optical compressibility on porosity, intrinsic refractive index of the  
 163 excipient and the API, and also API mass fraction. An expression for the linear two-variable  
 164 ( $f_{air}, x$ ) approximate effective refractive index of the tablet training sets of this study was given  
 165 in [25] as follows:

$$166 \quad n_{eff} = n_{MCC} - (n_{MCC} - 1)f_{air} - (n_{MCC} - n_{API})x \quad , \quad (8)$$

167  
 168 where  $n_{MCC}$  and  $n_{API}$  are the intrinsic refractive indices of MCC and Indomethacin,  $f_{air}$  is the  
 169 porosity of the tablet, and  $x$  is the dimensionless mass fraction (different from  $f_{API}$ ) of the API.  
 170 By substituting Eq. (8) into Eq. (7), the optical compressibility can be re-expressed as,

$$171 \quad \beta_{THz} = \frac{1}{(n_{MCC}-1)(1-f_{air})-(n_{MCC}-n_{API})x} \quad (9)$$

172 Since  $n_{MCC}$  and  $n_{API}$  are constants, it is evident from Eq. (9) that  $\beta_{THz}$  is inversely dependent  
 173 (hyperbolic dependence) on the porosity  $f_{air}$  or mass fraction  $x$  only when one of them is  
 174 constant. In a general case, both porosity and the dimensionless mass fraction are considered  
 175 to vary.

176 The optical compressibility  $\beta_{THz}$  depends on  $S$  via Eq. (5). If we compare Eqs. (6) and (7), the  
 177 message is pretty much similar. The thermodynamic compressibility  $\beta$  becomes less as the  
 178 pressure increases. In the case of increasing compression pressure in the tableting process the  
 179 porosity of the tablet is decreasing and the effective refractive index is increasing, thus resulting  
 180 in the decrease of  $\beta_{THz}$ . The optical compressibility parameter  $\beta_{THz}$  and its connection to the  $S$   
 181 structure parameter was studied for the training set of pharmaceutical tablets, and the results  
 182 obtained will be shown below.

183

## 184 **Materials and methods**

185 Two sets of round flat-faced pharmaceutical tablets were compressed from the defined  
 186 mixtures of pharmaceutical excipient MCC (Avicel PH101, FMC BioPolymer, Philadelphia,

187 USA) and API Indomethacin (Hangzhou Dayangchem Co. Ltd., Hangzhou, China). The widely  
188 used MCC is a typical hydrophilic excipient [21], the nominal particle size and true density of  
189 the particulate Avicel PH101 are 50  $\mu\text{m}$  and 1.55  $\text{g cm}^{-3}$ , respectively. The true density of the  
190 crystalline gamma polymorph of Indomethacin used in this study is 1.37  $\text{g cm}^{-3}$ . Two training  
191 sets of flat-faced tablets of constant diameter 13 mm were compacted using a compaction  
192 simulator (PuuMan, Kuopio, Finland). More details on the sample preparation of the tablets  
193 were described previously [26-28]. In Tables 1 and 2, various properties of the training tablet  
194 sets are presented. In tablet Set 1, porosity and API mass fractions were kept constant at ca. 36  
195 % and 10 wt%, respectively, whereas both were varied for the case of the tablet Set 2. For both  
196 tablet sets, five tablets were compressed for each sample number and the given values in Tables  
197 1 and 2 are the average values of 5 tablets belonging to a given tablet number. For each sample,  
198 statistical errors in the calculations made for the nominal porosities are as follows: diameter  $\pm$   
199 0.008 mm, height  $\pm$  0.005 mm (standard deviation of the sample mean), weight  $\pm$  0.01 mg  
200 (readability and sensitivity of the scale), effective refractive index  $\pm$ 0.002 (by assuming a  
201 temporal resolution of 0.02 ps) and porosity  $\pm$  0.2 % (calculated using the error propagation  
202 law).

203 Here we report on two case studies related to the lumped structural  $S$  parameter and the optical  
204 compressibility as follows: Case 1; fixed porosity and fixed API mass fraction but variable  
205 height, and Case 2; varied porosity, API mass fraction and height. To calculate the  $S$  parameter,  
206 presented in Tables 1 and 2, we have to utilise Eqs. (1) - (5). In order to solve Eqs. (3) and (4),  
207 we have to know the zero porosity refractive indices of  $n_{\text{MCC}}$  and  $n_{\text{API}}$ , namely,  $n_{\text{MCC}}=1.86$  and  
208  $n_{\text{API}}=1.73$ . The latter value of zero porosity estimate of the refractive index of  $n_{\text{API}}$  is a better  
209 estimate than the one given in [25]. The zero porosity estimates of the refractive index of MCC  
210 and API were obtained by the linear extrapolation technique method as used in [20, 25, 28].  
211 The density of the samples was calculated from the average dimensions and the average  
212 measured weight of the tablet. The tablet porosity was calculated by forming a ratio between  
213 the tablet density and the true density of MCC and Indomethacin, and the  $S$  parameter was  
214 calculated by using the equations given in the theory section. In Table 1, we have numbered  
215 the samples according to the order of the increase of the tablet height, not the order of increase  
216 of the effective refractive index.

217

218

219

220

221

222

223

224

225 Table 1: Data of tablet Set 1. The mean values of the diameter  $d$ , height  $H$ , weight  $W$ , porosity  
 226  $f_{\text{air}}$ , effective refractive index  $n_{\text{eff}}$ , API mass fraction wt% ( $x$ ) and calculated  $S$  parameter for  
 227 four samples are shown. Since the porosity for all of the tablet samples is known, it is possible  
 228 to calculate the volume fractions of MCC and API, as was discussed in [20].

Sample number (Set 1)	$d$ (mm)	$H$ (mm)	$W$ (mg)	$f_{\text{air}}$ (%)	$n_{\text{eff}}$	$x$ (wt%)	$S$
1	13.097	2.742	361.47	36	1.529	10	0.220
2	13.078	3.333	438.73	36	1.533	10	0.206
3	13.066	3.626	476.45	36	1.537	10	0.194
4	13.062	3.927	514.70	36	1.535	10	0.198

229

230 Table 2: Data of tablet Set 2. The values of the diameter  $d$ , height  $H$ , weight  $W$ , porosity  $f_{\text{air}}$ ,  
 231 effective refractive index  $n_{\text{eff}}$ , API mass fraction wt% ( $x$ ) and calculated  $S$  parameter for five  
 232 pharmaceutical tablets are shown.

Sample number (Set 2)	$d$ (mm)	$H$ (mm)	$W$ (mg)	$f_{\text{air}}$ (%)	$n_{\text{eff}}$	$x$ (wt%)	$S$
1	13.076	3.955	404.02	50	1.405	11.00	0.271
2	13.075	3.642	403.64	46	1.441	10.50	0.253
3	13.094	3.273	405.67	40	1.498	10.00	0.219
4	13.093	2.971	404.23	34	1.551	9.50	0.201
5	13.081	2.734	406.20	28	1.602	9.00	0.194

233

## 234 **Skeletal bulk modulus determination**

235 Mercury intrusion measurements were conducted using an Autopore V mercury porosimeter  
 236 (Micromeritics Instrument Corporation, Norcross, GA, U.S.A.). The maximum applied  
 237 pressure of mercury is 414 MPa, equivalent to a Laplace throat diameter of 4 nm. The  
 238 equilibration time at each of the increasing applied pressures of mercury is set to 20 s. The  
 239 tablets are measured as supplied.

240 By observing the behaviour under intrusion and extrusion at the highest pressures it is possible  
 241 to ascertain whether the sample displays the typical pore retention hysteresis or whether  
 242 mercury is extruded initially at equal volume to that during intrusion as a function of pressure.  
 243 If the latter occurs, then it is possible to conclude that the skeletal material is being elastically

244 compressed, and the gradient of the elastic response to pressure provides a measure of the  
 245 elastic bulk modulus of the skeletal material, i.e. the material bulk modulus of the pore wall  
 246 when compressed equally from all directions. If the extrusion, however, exceeds the intrusion  
 247 then the skeletal material is partially undergoing strong plastic deformation. The plastic  
 248 deformation, however, is generally impossible to quantify as it is convoluted with the usual  
 249 mercury retention hysteresis due to necking and filament snapping, and ink bottle behaviour.  
 250 Thus, correcting for the elastic behaviour in the data can be included in the overall data  
 251 correction during the mercury intrusion comprising the more commonly known effects of  
 252 compression of mercury and expansion of the penetrometer [1]. This is performed conveniently  
 253 using the software Pore-Comp (a software program developed by and obtainable from the  
 254 Environmental and Fluids Modelling Group, University of Plymouth, U.K.), in which the  
 255 following equation is applied:

$$256 \quad V_{\text{int}} = V_{\text{obs}} - \delta V_{\text{blank}} + \left[ 0.175(V_{\text{bulk}}^1) \log_{10} \left( 1 + \frac{P}{1820} \right) \right] - V_{\text{bulk}}^1 (1 - \Phi^1) \left( 1 - \exp \left[ \frac{(P^1 - P)}{M_{\text{ss}}} \right] \right) \quad (10)$$

257 where  $V_{\text{int}}$  is the volume of intrusion into the sample,  $V_{\text{obs}}$  the intruded mercury volume reading,  
 258  $\delta V_{\text{blank}}$  the change in the blank run volume reading,  $V_{\text{bulk}}^1$  the sample bulk volume at  
 259 atmospheric pressure,  $P$  the applied pressure,  $\Phi^1$  the porosity at atmospheric pressure,  $P^1$  the  
 260 atmospheric pressure and  $M_{\text{ss}}$  the bulk modulus of the solid sample [29].

## 261 **Results and discussion**

262 The values for the optical compressibility parameter,  $\beta_{\text{THz}}$ , for the case of Set 1 are shown in  
 263 Fig. 1 as a function of  $S$ . The porosity and API mass fraction were kept constant and only the  
 264 height of the tablets was increased in this Set 1, which causes an increase in the volume of the  
 265 tablet. The increase of the volume can be a probable reason for differences in arrangement of  
 266 the particles in the direction of the THz pulse propagation, and hence different values of the  
 267 lumped structural parameter  $S$ . From Table 1 it is evident that the refractive index of the tablets  
 268 vary only slightly, whereas much stronger variations can be observed for their structural  
 269 parameter  $S$ , sensitive to the series-parallel arrangement of constituents in the tablets.

270 Assuming that all the tablets of Set 1 have the same porosity and API wt%, the conclusion can  
 271 be drawn that a different share of series and parallel arrangement of the skeleton structure of  
 272 the tablets contributes to slightly different values of the effective refractive index, and that this  
 273 is manifested by a rather big change in the value of  $S$ . Therefore,  $S$  has a descriptor role  
 274 regarding also the compressibility of a tablet. Actually, the different heights of the nominally  
 275 similar tablets of Set 1 generate essentially different shares of series and parallel structures and,  
 276 hence, different values of  $S$ . In other words, the packing of API and MCC is different according  
 277 to the different tablet heights, and thus, compression.

278 For the samples in the case of Set 2 we repeated the same analysis procedure as above. Note  
 279 that in this case the samples follow a different numbering rule, to the extent that when the tablet  
 280 height is decreasing (the volume of the tablet becomes smaller) the effective refractive index  
 281 is increasing, as shown in Table 2. In Fig. 2 we plot the structural parameter as a function of  
 282 the porosity for Set 2. Here, dependence of the structural parameter  $S$  on the porosity suggests

283 a nonlinear relationship, which can be mathematically deduced from Eqs. (3) - (5). The range  
284 of variation of  $S$  in this case of Set 2 is ca. 0.194 - 0.271, which is much wider than for the case  
285 of Set 1, ca. 0.198 - 0.220. In the case of Set 2, porosity and API are both subject to being  
286 varied. A wider range of porosity change suggests also a wider range of the magnitude of the  
287 structural parameter  $S$ .

288 The optical compressibility parameter  $\beta_{\text{THz}}$  as a function of  $S$  for tablet Set 2 is shown in Fig.  
289 3. The optical compressibility  $\beta_{\text{THz}}$  is increasing with increasing  $S$ . The optical compressibility  
290 range of Set 2 is ca 1.66 - 2.47, which is wider than that of Set 1 ca. 1.86 -1.89. Since both the  
291 porosity and the API mass fraction have been changing in the situation of Set 2, it is necessarily  
292 more complex than in the case of Set 1.

293 Besides the correlation of  $\beta_{\text{THz}}$  with the parameter  $S$  we also studied the explicit dependence of  
294  $\beta_{\text{THz}}$  on  $f_{\text{air}}$  and  $x$  (shown in Figs. 4 and 5). Fig. 4 suggests a nonlinear, hyperbolic dependence  
295 of  $\beta_{\text{THz}}$  on  $f_{\text{air}}$ . This is consistent with the estimate given in Eq. (9), namely a hyperbolic  
296 dependence of  $\beta_{\text{THz}}$  on  $f_{\text{air}}$ . The data of Fig. 5 show apparently a weaker nonlinearity in respect  
297 to the dependence on  $x$ . However, if the mass fraction  $x$  would have a wider scale of variation,  
298 hyperbolic dependence of  $\beta_{\text{THz}}$  on  $x$  would also be expected.

299 Fig 6 shows the calculated optical compressibility parameter as a function of the measured  
300 mechanical parameter, namely skeletal bulk modulus. It is obvious that there is a correlation  
301 between the optical compressibility and the skeletal bulk modulus. The change of the optical  
302 compressibility is relatively strong as a function of the skeletal bulk modulus if we compare  
303 the samples 3-5 of this set 2, which present low porosity tablets with the lowest API loadings  
304 amongst the present samples.

305 The skeletal bulk modulus of the sample number 1 of Set 2 (Table 2) has the highest value and  
306 so the least compressible skeletal solid material of the five samples. This sample has the highest  
307 API loading, and so the ratio of API to compressible excipient is the highest. Sample number  
308 5 of Set 2 (Table 2) in turn has the most compressible skeletal material corresponding with the  
309 lowest API loading. The API, therefore, has a high material bulk modulus, and in ratio with the  
310 more compressible excipient determines the observed compressibility of the tablet structure.

## 311 **Conclusions**

312 Compressibility of a pharmaceutical tablet is an important tablet property. The problem of  
313 measuring compressibility of a tablet is challenging because one needs to detect the change in  
314 volume of a tablet as a function of the compression pressure. This means, typically, that special  
315 measurement arrangements have to be realised under well-controlled laboratory conditions.  
316 Our idea outlined in this paper is to retrieve information on compressibility and, hence,  
317 mechanical properties of a tablet using a non-destructive method based on the THz pulse delay  
318 detection. In this article, we have introduced the concept of optical compressibility of  
319 pharmaceutical tablets.

320 The optical compressibility was studied for two training tablet sets. A theoretical model that  
321 gives explicit dependence of the optical compressibility of porosity and API mass fraction was  
322 given. The tablets of two differently compressed sets consisted of one excipient, MCC, and one

323 API, Indomethacin. For the purpose of describing their compressibility, we derive the concept  
324 of optical compressibility based on the effective refractive index of a tablet. The difference  
325 between the conventional and optical compressibility is that in the latter case there is, in  
326 principle, no longer a need to evaluate physical compressibility by detection of any pressure-  
327 induced volume change of the tablet. However, there is a valuable subtlety arising from the  
328 change in packing structure as a function of unidirectional compression. This is seen in a  
329 change of the parallel to series coordination of the skeletal material as monitored by the lumped  
330 parameter structure factor  $S$ . Thus, it is possible to derive a compressibility using the optical  
331 approach, and that this optical compressibility is unique to the excipient-API formulation ratio  
332 in that the compression of the tablet leads to a change in effective refractive index together  
333 with a unique packing change. Thus, the combination of  $n_{\text{eff}}$  and  $S$  as a function of compressive  
334 force provides a quality control tool for both tablet compression and formulation consistency.  
335 The transmitted terahertz signal, therefore, gives volumetric and structural information on the  
336 tablet as it stands without using any external disturbance. In other words, the optical  
337 compressibility is an intrinsic property of each tablet and its formulation.

338 Relatively regular behaviour of the optical compressibility as a function of the structural  
339 parameter,  $S$ , porosity  $f_{\text{air}}$ , and API mass fraction  $x$ , was obtained for both tablet Sets 1 and 2.  
340 Using the data of skeletal bulk modulus of Set 2 we found a correlation between the optical  
341 compressibility and bulk modulus. The bulk modulus relates only to the direct compressibility  
342 of the material itself making up the skeleton but not that of the skeleton structure.

343 The study of the structural parameter, as well as the optical compressibility provides a more  
344 comprehensive picture of the properties of a pharmaceutical tablet, and in principle can be used  
345 to understand better the mechanical properties such as strain, Young's modulus, Poisson's ratio  
346 etc. of a tablet.

347 Finally, we wish to remark that both the lumped structural parameter as well as the optical  
348 compressibility are suggested to be proportional to the surface roughness of a tablet [21]. It  
349 was demonstrated previously that the effective refractive index of tablets is proportional to the  
350 measured average surface roughness. This observation may open new ways to predict various  
351 properties of tablets by terahertz measurements in reflection setting, i.e. reflection of the THz  
352 pulse. Such a concept would be particularly beneficial when the API or excipient strongly  
353 absorbs THz radiation, rendering transmission measurements unfeasible.

354

## 355 **References**

- 356 [1]. M. E. Aulton, "*Pharmaceutics the science of dosage from design*", 2<sup>nd</sup> Edn. ,Churchill  
357 Livingstone, Edinburgh, 2002.
- 358 [2]. H. Lieberman, L. Lachman, J. B. Schwartz, "*Pharmaceutical Dosage Forms Tablets*",  
359 Vol. 3, 2<sup>nd</sup> Edn. Marcel Dekker, New York, 1990.
- 360 [3]. F. P. Knudsen, "*Dependence of Mechanical Strength of Brittle Polycrystalline*  
361 *Specimens on Porosity and Grain Size*", J. Am. Ceram. Soc., 42, 376 – 387, 1959.

- 362 [4]. R. M. Spriggs, “*Expression for effect of porosity on elastic modulus of polycrystalline*  
363 *refractory materials*”, particularly aluminium oxide, J. Am. Ceram. Soc., 44, 628 - 629,  
364 1961.
- 365 [5]. J. T. Fell, J. M. Newton, “*Determination of tablet strength by the diametral-*  
366 *compression test*”, J. Pharm. Sci., 59, 688 – 691, 1970.
- 367 [6]. G. Alderborn, Tablets and compaction. In: Aulton, M.E. (Eds), “*Pharmaceutics the*  
368 *Science of Dosage Form Design, 2<sup>nd</sup> Edn.* Churchill Livingstone, Edinburgh, 2002.
- 369 [7]. J. A. Choren, S. M. Heinrich, M. B. Silver-Thorn, “*Young’s modulus and volume*  
370 *porosity relationships for additive manufacturing applications*”, J. Mat. Sci., 48, 5103  
371 - 5112, 2013.
- 372 [8]. K. E. Peiponen, P. Bawuah, M. Chakraborty, M. Juuti, J. A. Zeitler and J. Ketolainen  
373 “*Estimation of Young’s modulus of pharmaceutical tablet obtained by terahertz time-*  
374 *delay measurement*”, Int. J. Pharm, 2015.
- 375 [9]. D. Zhou, Y. Qiu, “*Understanding Material Properties in Pharmaceutical Product*  
376 *Development and Manufacturing: Powder Flow and Mechanical Properties*”, J. Valid.  
377 Techn., 65 - 77, 2010.
- 378 [10]. C. K. Tye, C. (Calvin) Sun, G. E. Amidon, “*Evaluation of the effects of tableting*  
379 *speed on the relationships between compaction pressure, tablet tensile strength, and*  
380 *tablet solid fraction*”, J. Pharm. Sci., 94, 465 – 472, 2005.
- 381 [11]. A. Hart, “*Effect of Particle Size on Detergent Powders Flowability and Tabletability*”,  
382 Chem. Eng. Process Techn., 6, 1- 4,2015.
- 383 [12]. R. W. Heckel, “*Density-pressure relationship in powder compaction*”, Trans. Metall.  
384 Soc. AIME, 221. 671 - 675. 1961.
- 385 [13]. H. Leuenberger, B. D. Rohera, “*Fundamentals of Powder Compression. I. The*  
386 *Compactibility and Compressibility of Pharmaceutical Powders*”, Pharm. Res., 3, 12 -  
387 22, 1986.
- 388 [14]. R. Ishino, H. Yoshino, Y. Hirakawa, K. Noda, “*Influence of tableting speed on*  
389 *compactibility and compressibility of two direct compressible powders under high*  
390 *speed compression*” Chem. Pharm. Bull., 38, 1987 - 1992, 1990.
- 391 [15]. S. Patel, A. M. Kaushal, A. K. Bansal, “*Effect of Particle Size and Compression Force*  
392 *on Compaction Behavior and Derived Mathematical Parameters of Compressibility*”,  
393 Pharm. Res., 24, 111 - 124, 2007.
- 394 [16]. D. H. Choi, N. A. Kim, K. R. Chu, Y. J. Jung, J-H. Yoon, S. H. Jeong, “*Material*  
395 *Properties and Compressibility Using Heckel and Kawakita Equation with Commonly*  
396 *Used Pharmaceutical Excipients*”, J. Pharm. Inv., 40, 237 - 244, 2010.

- 397 [17]. K. S. Khomane, P. K. More, G. Raghavendra, A. K. Bansal “*Molecular*  
398 *Understanding of the Compaction Behavior of Indomethacin Polymorphs*”, Mol.  
399 Pharm., 10, 631-639, 2013.
- 400 [18]. I. M. Hamad, A. M. A. Salman, S. Elkarib, W. A. M. A. Salman, “*The Effect of Particle*  
401 *Size on Compressibility of Cinnamon Granules*”, J. Appl. Indust. Sci., 3, 150 - 153,  
402 2015.
- 403 [19]. K. E. Peiponen, J. A. Zeitler, M. Kuwata-Gonokami (Eds.) *Terahertz Spectroscopy and*  
404 *Imaging* (Springer, Berlin, 2013).
- 405 [20]. P. Bawuah, M. Chakraborty, T. Ervasti, J. A. Zeitler, J. Ketolainen, P. A.C. Gane. K.  
406 -E Peiponen, “*A structure parameter for porous pharmaceutical tablets obtained with*  
407 *the aid of Wiener bounds for effective permittivity and terahertz time-delay*  
408 *measurement*”, Int. J. Pharm, 506, 87 – 92, 2016.
- 409 [21]. M. Chakraborty, P. Bawuah, Nicholas Tan, T. Ervasti, P. Pääkkönen, J. A. Zeitler, J.  
410 Ketolainen, K-E. Peiponen, “*On the Correlation of Effective Terahertz Refractive*  
411 *Index and Average Surface Roughness of Pharmaceutical Tablets*” J Infrared Milli  
412 Terahz Waves, DOI 10.1007/s10762-016-0262-0, 2016.
- 413 [22]. D. E. Aspnes, “*Local-field effects and effective medium theory: A microscopic*  
414 *perspective*”, Am. J. Phys., 50,704-709 ,1982.
- 415 [23]. O. Krischer, W. Kast, *Die Wissenschaftlichen Grundlagen der Trocknungstechnik.*  
416 (Springer, Berlin, 1978).
- 417 [24]. O. A. Adetunji, M. A. Odeniyi, O. A. Itiola, “*Compression, Mechanical and Release*  
418 *Properties of Chloroquine Phosphate Tablets containing corn and Trifoliolate Yam*  
419 *Starches as Binders*”, Trop. J. Pharm. Res., 5 ,589 - 596, 2006.
- 420 [25]. P. Bawuah, N.Tan, S. N. A. Tweneboah, T. Ervasti, J. Ketolainen, J. A. Zeitler, K. E.  
421 Peiponen, “ *Terahertz study on porosity and mass fraction of active pharmaceutical*  
422 *ingredient of pharmaceutical tablets*”, Eur. J. Pharm. Biopharm. 105, 122 – 133, 2016.
- 423 [26]. T. Ervasti, P. Silfsten, J. Ketolainen, K. E. Peiponen, “*A study on the resolution of a*  
424 *Terahertz Spectrometer for the assessment of the porosity of pharmaceutical tablets*”,  
425 Appl. Spectrosc., 66, 319 - 323, 2012.
- 426 [27]. P. Bawuah, A. Pierotic Mendia, P. Silfsten, P. Pääkkönen, T. Ervasti, J. Ketolainen, J.  
427 A. Zeitler, K. E. Peiponen, “*Detection of porosity of pharmaceutical compacts by*  
428 *terahertz radiation transmission and light reflection measurement techniques*”, Int. J.  
429 Pharm., 465, 70 - 76, 2014.
- 430 [28]. P. Bawuah, P. Silfsten T. Ervasti, J. Ketolainen, J. A. Zeitler, K-E Peiponen, “*Non-*  
431 *contact weight measurement of flat-faced pharmaceutical tablets using terahertz*  
432 *transmission pulse delay measurements*”, Int. J. Pharm., 476, 16 – 22, 2014.

433 [29]. P.A.C. Gane, J.P. Kettle, G.P. Matthews, C.J. Ridgway, *Void Space Structure of*  
434 *Compressible Polymer Spheres and Consolidated Calcium Carbonate Paper-Coating*  
435 *Formulations*, Ind. Eng. Chem. Res., 35, 1753-1764, 1996.

436

437

438

439

Figure captions

Fig. 1: Optical compressibility  $\beta_{\text{THz}}$  as a function of structural parameter  $S$  for Set 1.

Fig. 2: Structural parameter  $S$  as a function of porosity  $f_{\text{air}}$  for Set 2.

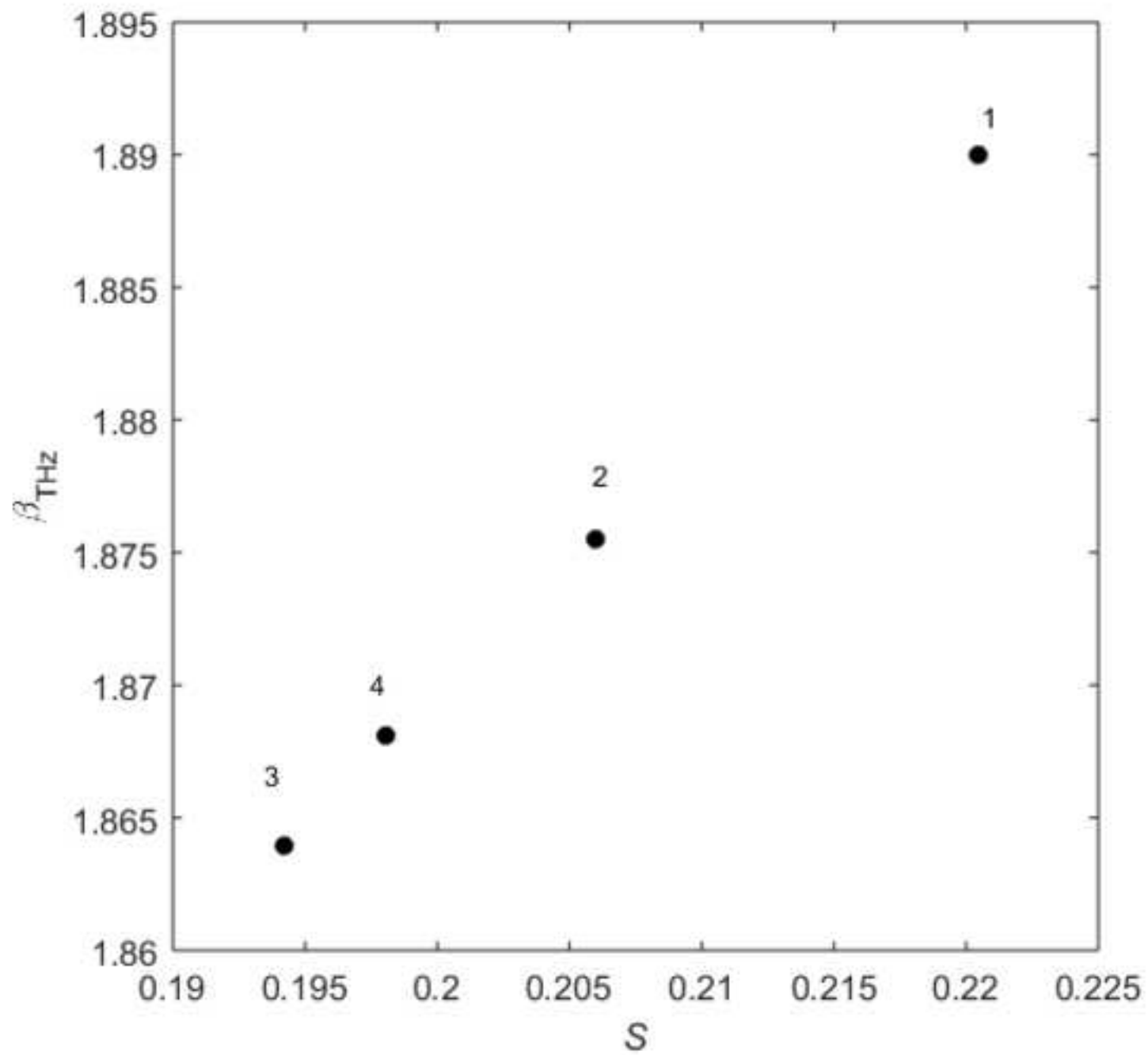
Fig. 3: Optical compressibility  $\beta_{\text{THz}}$  as a function of structural parameter  $S$  for Set 2

Fig. 4: Optical compressibility  $\beta_{\text{THz}}$  as a function of porosity  $f_{\text{air}}$  for Set 2.

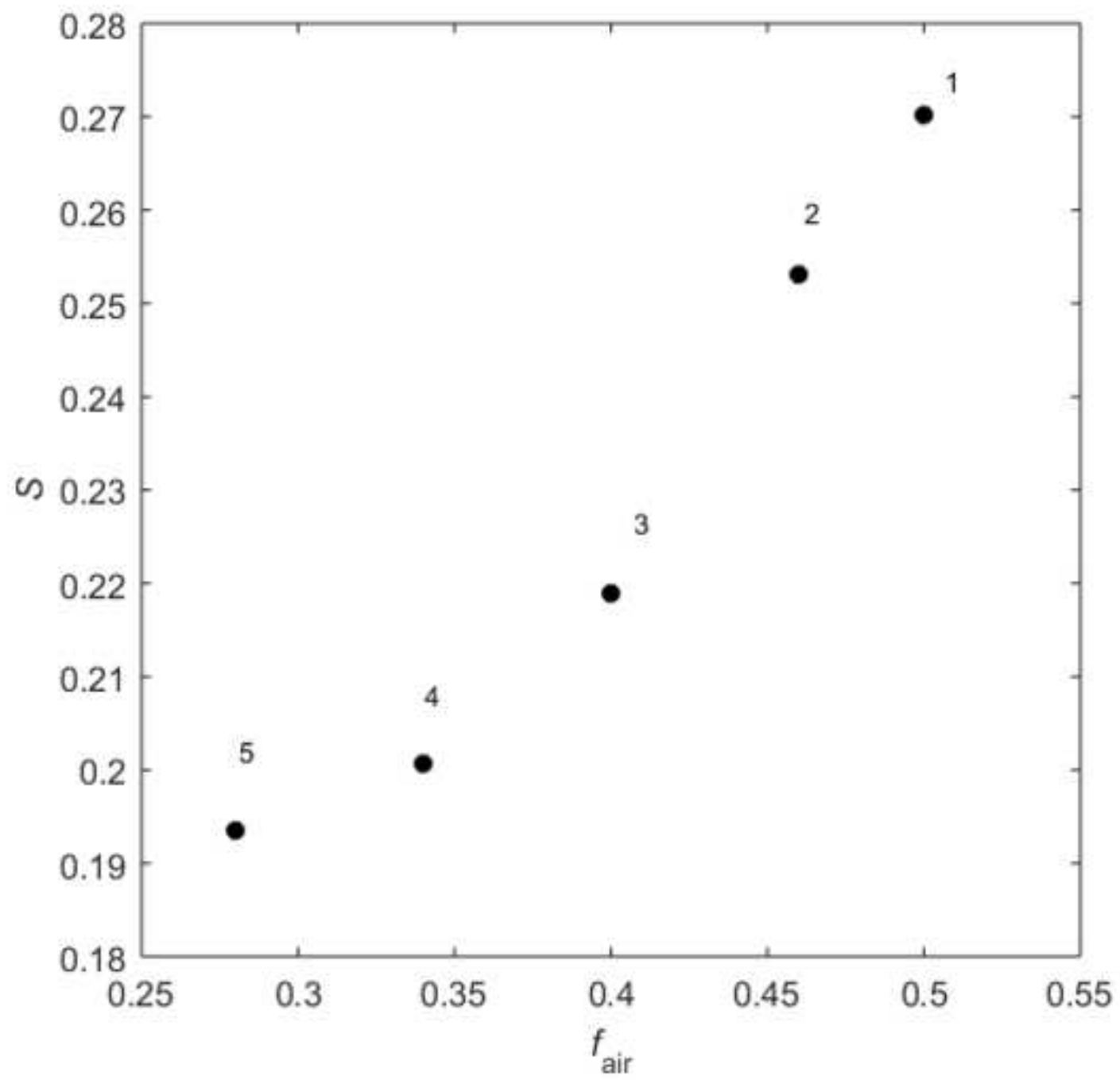
Fig. 5: Optical compressibility  $\beta_{\text{THz}}$  as a function of mass fraction  $x$  for Set 2.

Fig. 6: Optical compressibility  $\beta_{\text{THz}}$  as a function of Bulk modulus  $M_{\text{ss}}$  for Set 2.

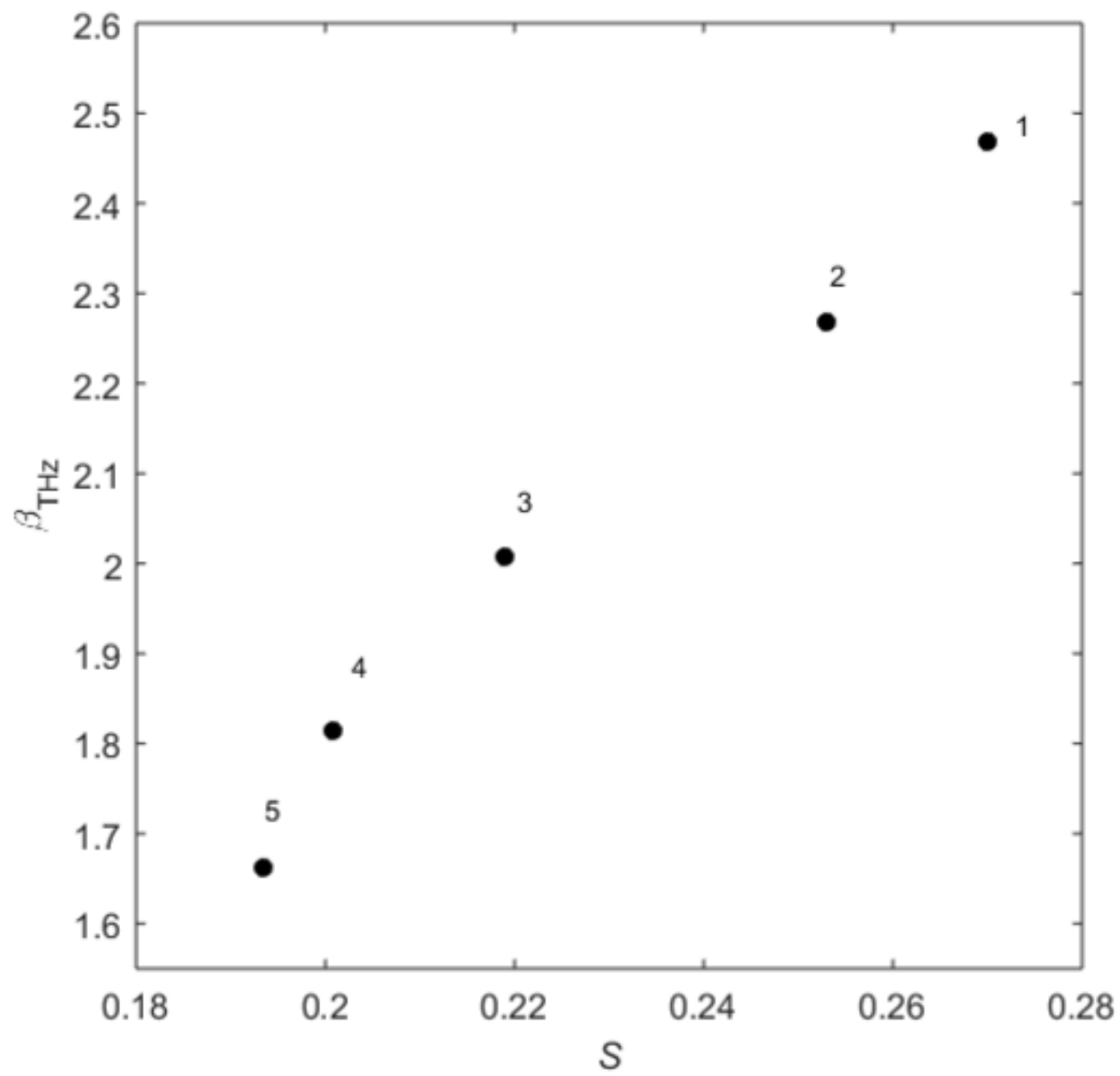
Figure(1)



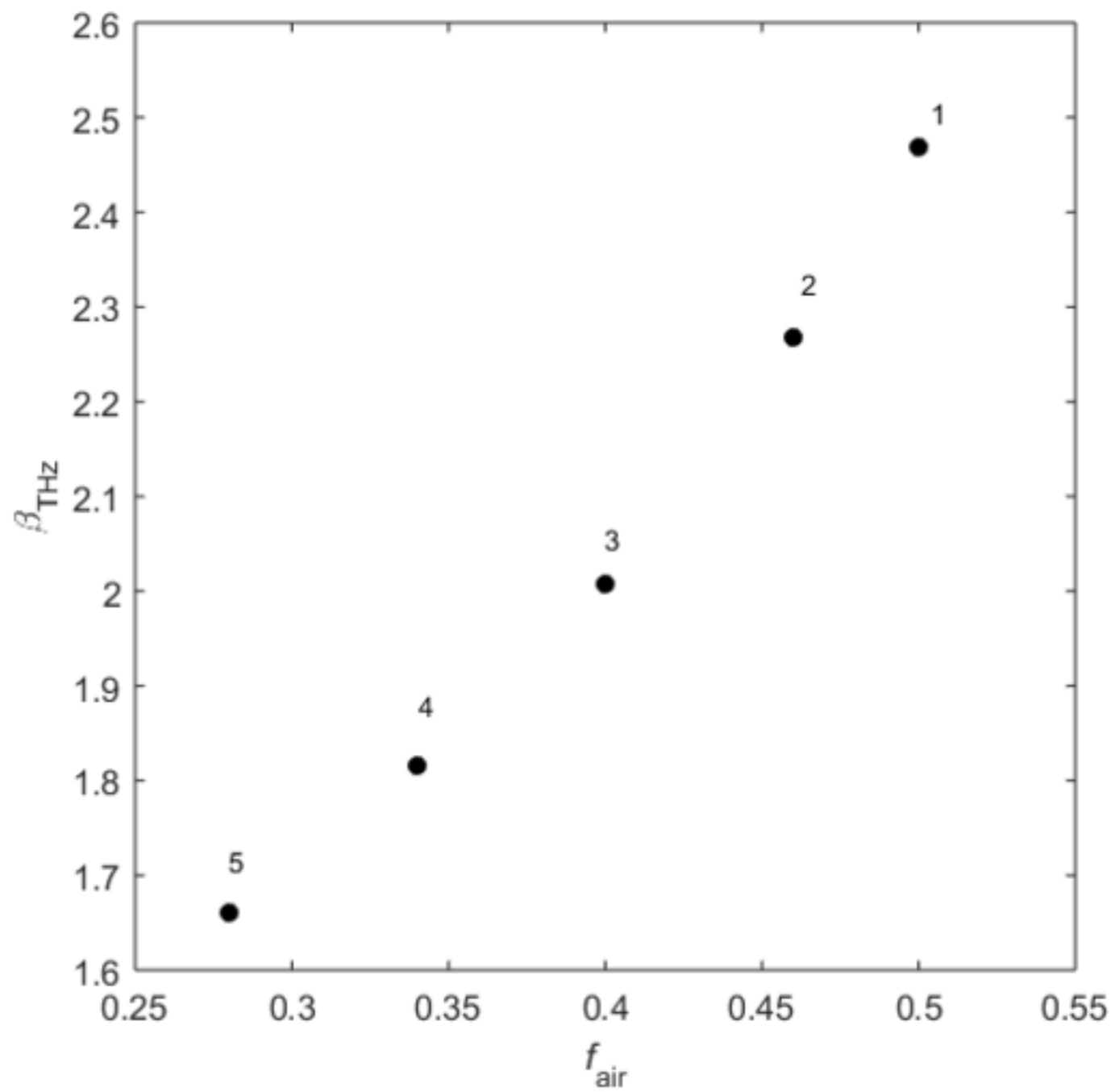
Figure(2)



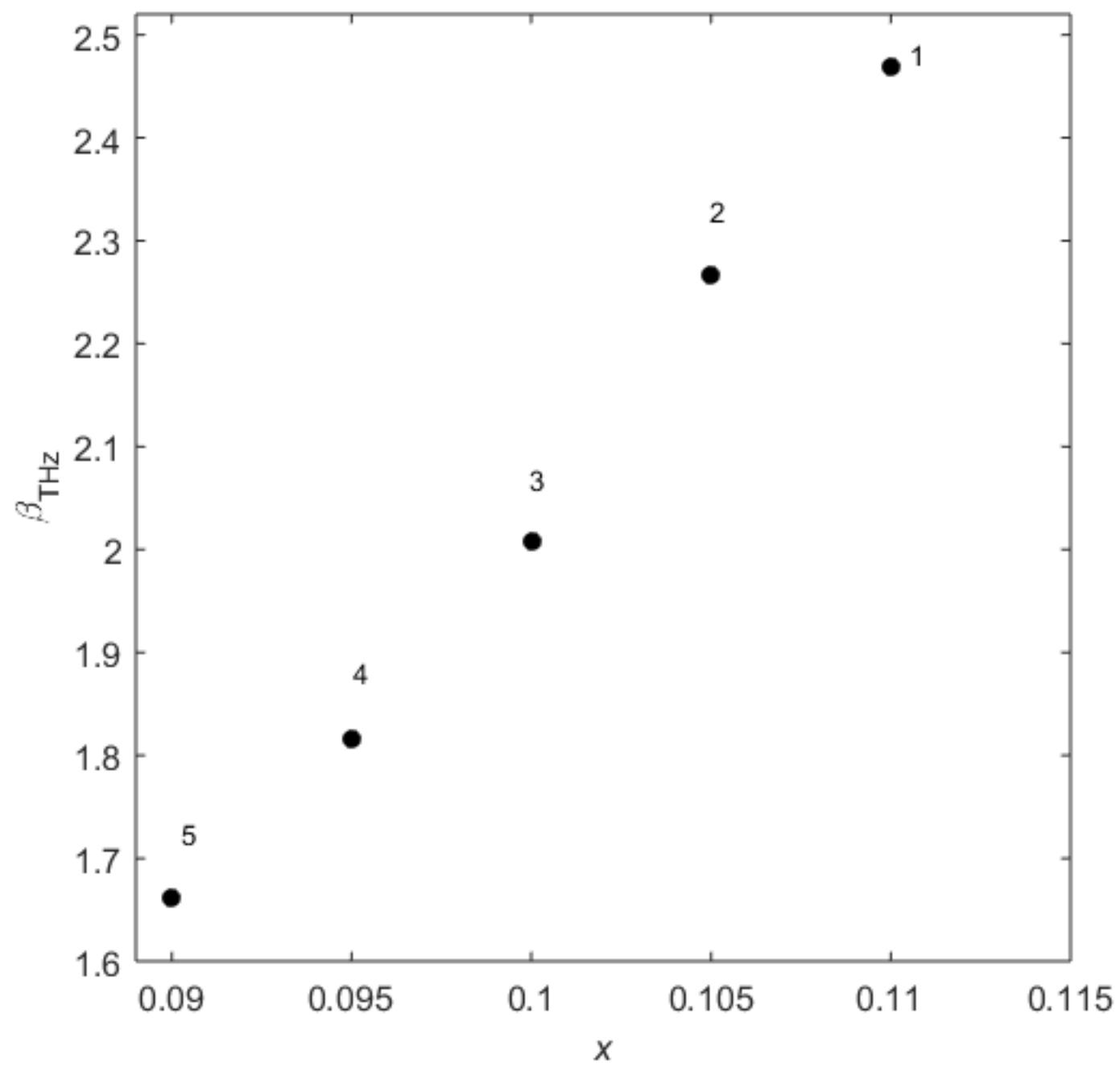
Figure(3)



Figure(4)



Figure(5)



Figure(6)

